Shot peening and deep cold rolling of a single crystal nickel superalloy

I. Bogachev[1], K.M. Knowles[1], G. Gibson[2]

[1] University of Cambridge, Department of Materials Science and Metallurgy, 27 Charles Babbage Road, Cambridge, CB3 0FS, UK – ib358@cam.ac.uk, kmk10@cam.ac.uk
[2] Rolls-Royce plc, PO Box 31, Derby, DE24 8BJ, UK – grant.gibson@rolls-royce.com

Abstract
The present research aims to further the understanding of the effects of mechanical shot peening (MSP) and deep cold rolling (DCR) on the single crystal nickel-based superalloy CMSX-4, used in the manufacture of jet engine turbine blades. Under the thermomechanical conditions of a turbine, the main resistance to fatigue crack growth is thought to come from the surface cold work generated by these procedures. Cold work in samples treated by MSP or DCR was characterised by scanning electron microscopy, both in the as-hardened state and following heat treatment at 900 and 1100 °C. Centre hole drilling was used to find the depths of residual stress also induced by the procedures. DCR was found to produce a deeper layer of relatively low cold work in comparison with MSP. Slip bands were induced by both procedures and were especially dense following MSP. After heat treatment at 900 °C for 500 h, topologically close-packed precipitates formed on slip bands, and discrete recrystallisation occurred in the cold worked layer, with little or no recovery. At 1100 °C for 100 h, complete surface recrystallisation was observed in both samples. DCR resulted in shallower recrystallisation in both cases. The microstructures of both samples underwent rafting at 1100 °C, with the depth levels of the rafting below the surface correlating with the depth levels of compressive residual stress, both being significantly greater than cold work depths.

Keywords: *nickel-based superalloys, single crystal, mechanical shot peening (MSP), deep cold rolling (DCR)*

Introduction

There is rising interest in the aerospace industry in using surface hardening techniques, such as mechanical shot peening (MSP) and deep cold rolling (DCR), to improve the fatigue resistance of jet engine turbine blades. Traditionally optimised to resist creep, turbine blades are typically manufactured from single crystal nickel-based superalloys, which possess excellent creep resistances and high-temperature strengths. These properties are due to an ordered precipitate phase, often the γ' phase, which forms cube-shaped precipitates inside the γ matrix phase and can make up as much as 70 vol% of the material [1].

DCR, in which the surface of a sample is systematically rolled with a hard roller under hydrostatic pressure, is known to produce deeper residual stresses and a better surface finish than MSP. However, DCR is more challenging to apply to complex sample geometries [2].The effects of MSP and DCR on polycrystalline superalloys have been widely studied [3,4], but their effects on the single crystal blade alloys are less well understood.

Surface hardening procedures are known to induce a layer of cold work and a residual compressive stress at the surface of the material. In high stress, high temperature environments, such as in a turbine, the cold worked layer is thought to play the chief role in increasing the resistance to fatigue crack growth [5,6]. The present work, therefore, is concerned primarily with characterising the cold work produced in samples of a single crystal superalloy prior to their use in a high stress, high temperature environment. The microstructures of two samples, treated by DCR or MSP, are analysed and compared, both in the as-hardened state, and following heat treatments at 900 or 1100 °C.

Experimental Methods

Samples of the superalloy CMSX-4 were cast and machined into square cross-section rods, with surface hardening performed on each long face of a sample. One sample was treated by MSP using 110H shot, 0.20–0.25 mmA intensity and 1600 % coverage. Another sample underwent DCR with a 6 mm diameter roller at 30 MPa pressure. Sections of these samples were subjected to two different heat treatments under vacuum, with no externally applied stress: 900 °C for 500 h or 1100 °C for 100 h.

Scanning electron microscopy was performed on sample cross-sections using a Zeiss GeminiSEM 300. Microstructures were examined using backscattered electron imaging. Surface cold work was studied using electron backscattered diffraction (EBSD). Local variations in material crystallographic orientation are dependent on dislocation density, and therefore on the degree of cold work. By calculating these local variations for each pixel in an EBSD scan, maps showing the distribution of cold work in each sample were plotted. The kernel average neighbour misorientation (KANM) parameter [7] (3×3 kernel), in degrees of misorientation, was used to perform this quantification. Depths of cold work were found by plotting profiles of average KANM against depth in each map and finding where this became less or equal to a far-field baseline value, as detailed in ref. 8.

Centre hole drilling (CHD) was used to assess the depths of compressive residuals stresses. It should be noted that current CHD methodology is not adapted to single crystal materials, and therefore stress magnitudes should be not be viewed as quantitative.

Experimental Results

As-hardened material

Significant cold work was produced by both DCR and MSP in the surfaces of the samples (Figure 1), causing a layer of heightened KANM at the surface (Figures 1a and 1b), and bulk variations in material orientation, revealed through channelling contrast (Figures 1d and 1e). The average amount of cold work decreased more or less monotonically with depth in both samples, down to a bulk baseline (Figure 1c).

Average cold work depths were measured to be 330 ± 14 and 107 ± 10 μm for the DCR and MSP samples, respectively. However, cold work in the MSP sample was of a greater magnitude, with a denser set of slip bands. This is evident from comparisons of Figures 1a and 1b, and of Figures 1c and 1d. Numerically, this is shown by the average increase in KANM per depth within the cold worked layer in both samples – 0.26 ± 0.05 and 0.74 ± 0.07 °/μm, respectively. Significant lateral variations in local cold work were also observed in both samples. In DCR, in particular, deformation can be seen to be concentrated in narrow streaks on the surface.

Heat treatment at 900 °C for 500 h

Samples were heat treated at 900 °C for 500 h; this is similar to the total time a superalloy would spend at this temperature in service. The nominal depths of cold work were found to be unaffected by the heat treatment: 340 ± 20 and 108 ± 13 μm in the DCR and MSP samples, respectively. Similarly, no recovery of the bulk cold work was observed in either sample, as shown by the similar KANM values in Figures 1 and 2.

However, recrystallisation (RX) – the formation of new grains with a lower dislocation density [9] – within the cold worked layer was observed. RX grains are seen in KANM maps as dark areas on the surfaces of both samples (Figures 2a and 2b). Large RX grains containing a developed γ/γ' structure are also distinguishable in BSE images (Figure 2e). The maximum depth of RX, which determines to what depth the resistance to fatigue damage provided by the cold work is undermined, was considerably greater in the MSP sample than in the DCR sample – 24 and 8 μm, respectively, despite the latter sample having a much greater cold work depth. This is due to the greater magnitude of cold work in the MSP sample, which provides more driving force and faster diffusion for RX grains to form.

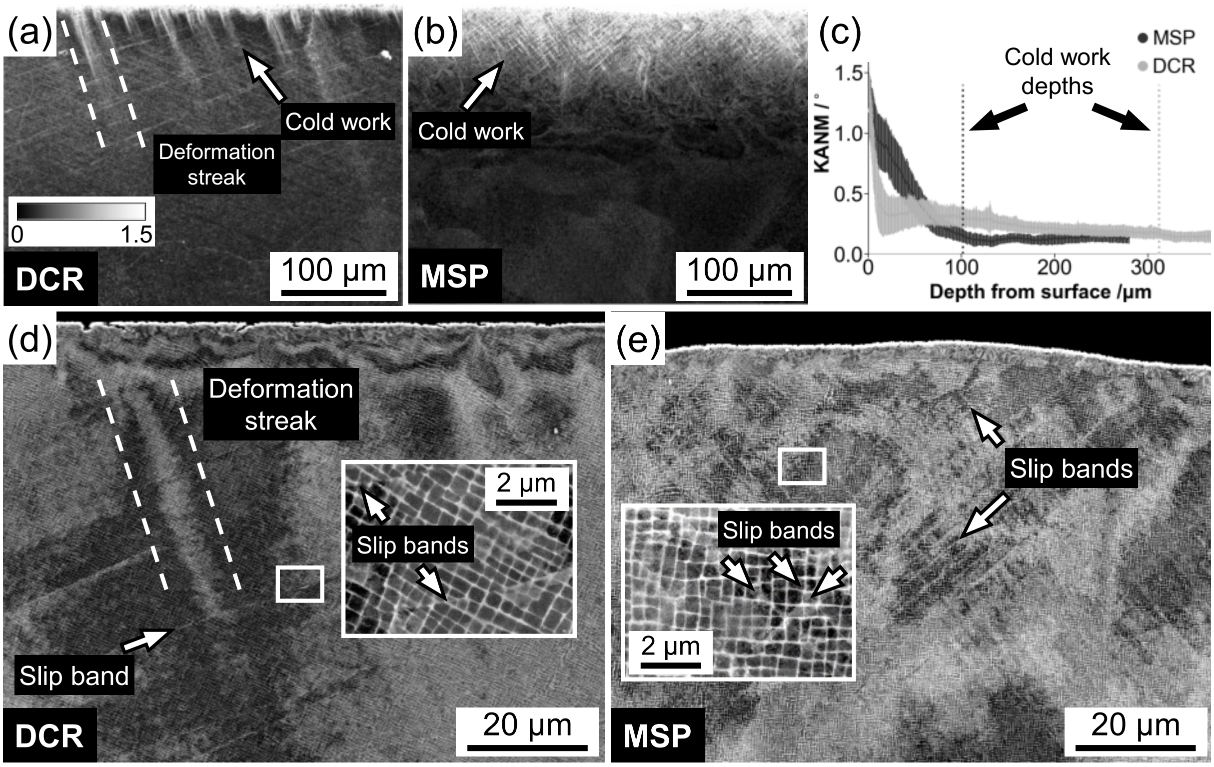

Figure 1: *As-hardened DCR and MSP samples. (a), (b) are KANM maps, with depth profiles of these maps plotted in (c). Sample microstructures are shown in (d), (e). The white boxes give the scales of the enlarged microstructure views, in which γ' is darker and γ is lighter.*

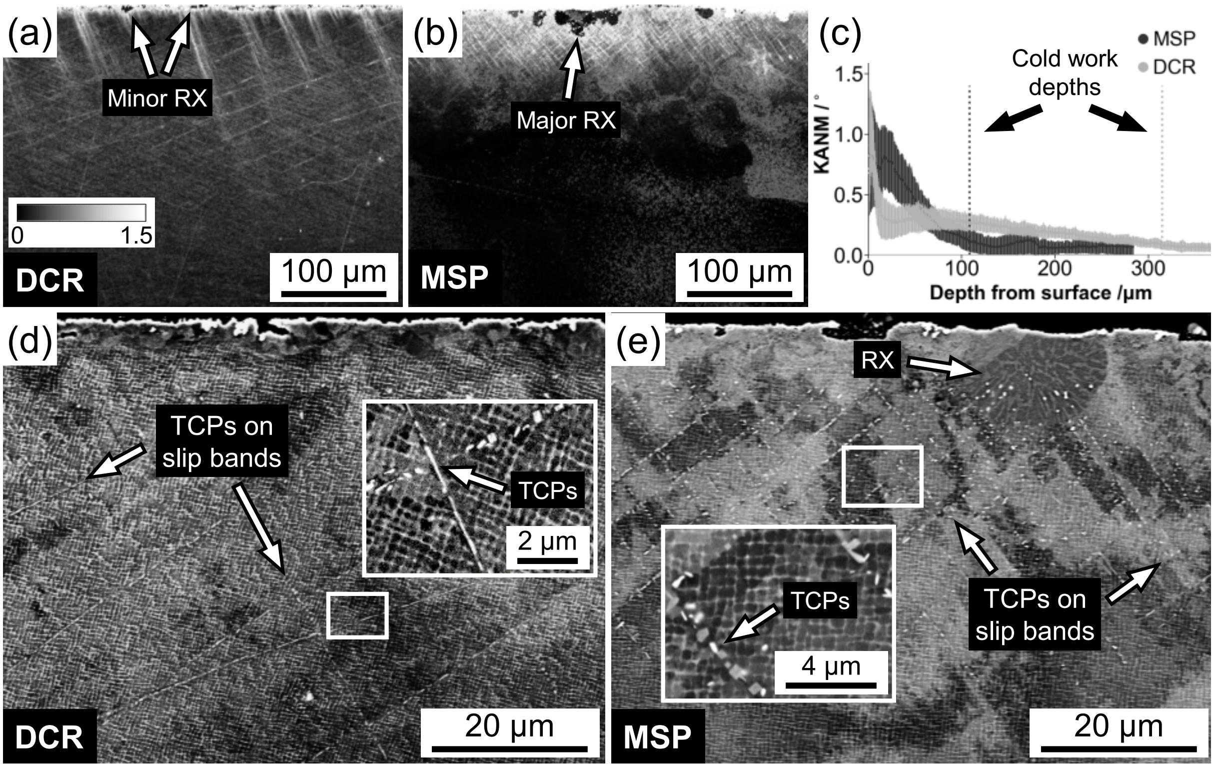

Figure 2: *DCR and MSP samples after 500 h at 900 °C. (a), (b) are KANM maps, with depth profiles of these maps plotted in (c). Sample microstructures are shown in (d), (e). The white boxes give the scales of the enlarged microstructure views.*

Precipitation of topologically close-packed (TCP) phases was observed in both samples (Figures 2d and 2e). These phases are rich in heavy alloying elements and can act as crack nucleation sites [10]. Their formation was seen to begin after just 10 h of heat treatment (images not shown). Superalloys are designed to be kinetically stable with respect to TCP precipitation, and slip bands clearly played a key role in their formation in the present samples. TCPs, seen in Figures 2d and 2e lying predominantly in straight lines, clearly adhere closely to slip bands. TCPs were slightly larger in the DCR sample than in the MSP sample (partly due to their greater elongation, see Figure 2d), with average sizes of 0.30 ± 0.06 and 0.24 ± 0.03 µm, respectively, but were much more sparse in the DCR sample, in which the density of slip bands is lower. TCPs formed up to depths of ~160 and ~60 µm in the DCR and MSP samples, respectively, roughly coinciding with the depths to which slip bands could be visibly distinguished in each sample.

Heat treatment at 1100 °C for 100 h

To test the response of the cold work in a more extreme environment, the two samples were heat treated at 1100 °C for 100 h. In both samples, this promoted the formation of RX grains across the entire sample surfaces, to a greater depth than after 500 h at 900 °C, with the MSP sample again having deeper RX than the DCR sample (Figures 3a and 3b). Indeed, most of the cold worked layer in the MSP sample recrystallised, leaving only a lip of remnant cold work. After this heat treatment, the DCR sample now actually had greater cold work magnitudes at all depths (Figure 3c).

This heat treatment also resulted in rafting – the directional coarsening of γ' precipitates, forming elongated plates or “rafts” (Figure 3d). Rafting is known to occur in single crystal superalloys under an applied external stress, but reports of rafting following surface treatments are rarer [11].

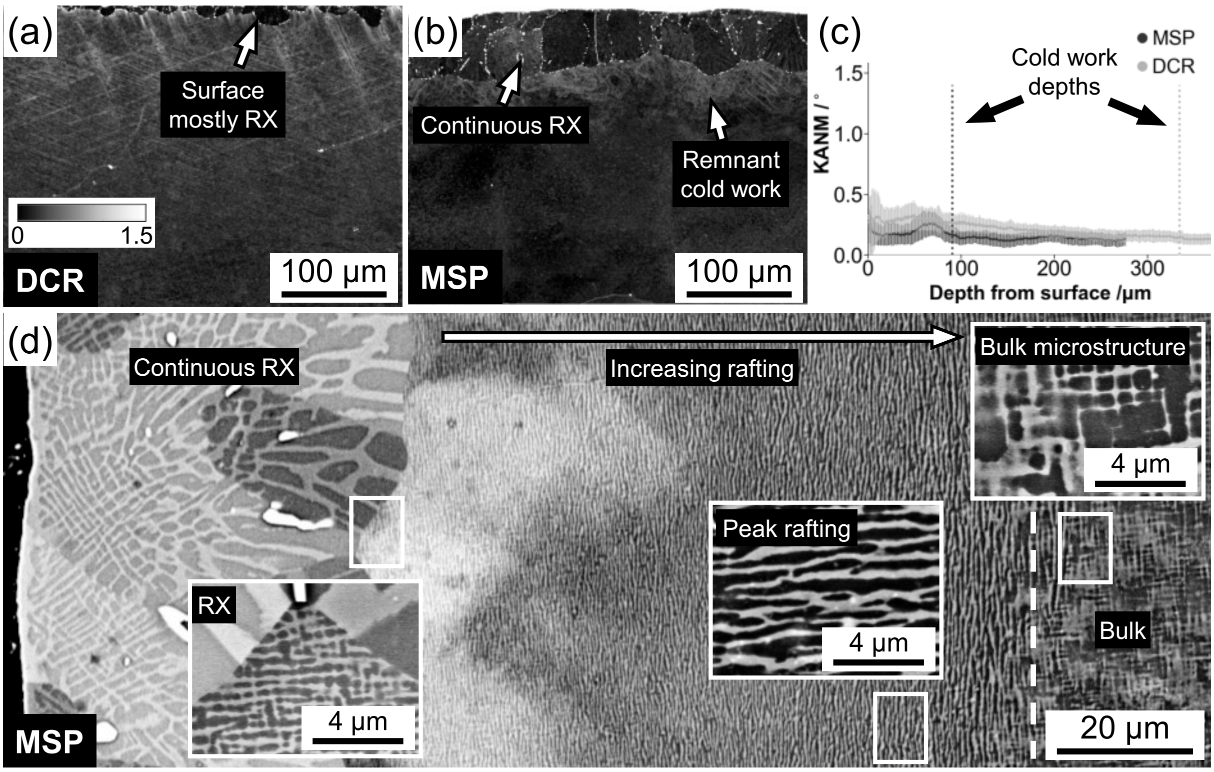

***Figure 3**: DCR and MSP samples after 100 h at 1100 °C. (a), (b) are KANM maps, with depth profiles of these maps plotted in (c). Sample microstructures are shown in (d), (e). The white boxes give the scales of the enlarged microstructure views.*

The extent of rafting, characterised by the “raft ratio” – the ratio of the average lengths of straight raft segments parallel and perpendicular to the raft direction – is plotted against depth for the two samples in Figure 4a. A raft ratio of 1 indicates an unrafted material state where the γ' precipitates have sides of equal length. In both samples, the degree of rafting increased with depth, reaching peak values of ~2.5–3, and then decreased again to ~1, when the material adopted a bulk microstructure (compare this with Figure 3d).

Since rafting behaves in an opposite sense to cold work, which decreases monotonically from a maximum at the surface, it must be occurring under the influence of the residual compressive stresses generated by MSP and DCR. It is known that rafting may continue, once initiated, even if the stress is subsequently removed [12]; therefore any relaxation of the residual stress does not mean rafting would cease. Depths of compressive residual stresses were obtained from residual stress profiles for the two samples, measured by CHD (Figure 4b; magnitudes not quantitative: see Experimental Methods). The depths of cold work, peak rafting, total rafting and compressive residual stress for both samples are given in Table 1.

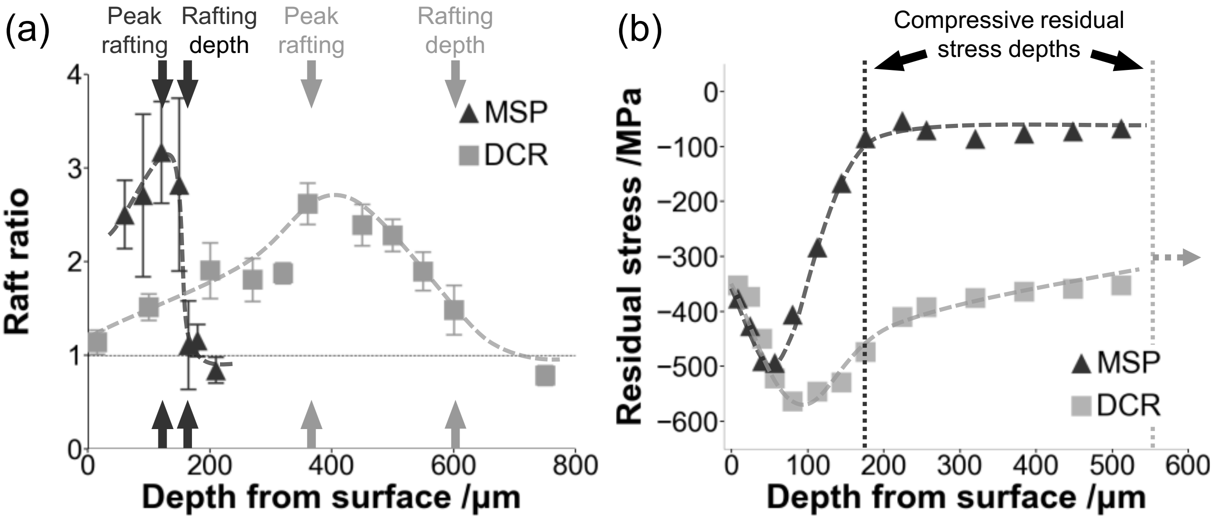

Figure 4*: (a) Extent of rafting versus depth in MSP and DCR samples after 100 h at 1100 °C, with peak rafting and total rafting depths marked for each sample. (b) Residual stress profiles for each sample in the as-hardened state. Compressive residual stress depth for the DCR sample is outside the measured range*

Sample	Cold work depth	Peak rafting depth	Rafting depth	Compressive residual stress depth
MSP	107	120	165	176
DCR	330	360	600	>500

Table 1*: As-hardened cold work depths and compressive residual stress depths, and peak and total rafting depths after 100 h at 1100 °C, in μm, in the DCR and MSP samples.*

In both samples, it can be seen that peak rafting occurs beyond the depth of cold work, whereas the total raft depth correlates fairly well with the depth of compressive residual stress. From this, it seems that cold work actually hinders rafting, which is instead driven by the surface compressive residual stresses.

This observation also highlights the fact that the depths of compressive residual stress and cold work do not have to coincide. Residual stress arises from a macroscopic change of the sample shape, whereas cold work is the microscopic change in the material microstructure, resulting in greater dislocation density. The EBSD method measures the depth to which there is a significant increase in dislocation density. However, it can be used to set a lower bound on the depth of compressive residual stress. This is because the depth of the deformed plastic layer below the surface will be equal to or greater than the depth below the surface of the layer where there is a significant increase in dislocation density relative to the base material.

Conclusions

A comparison has been made of the cold work and microstructures of samples of a single crystal superalloy treated by MSP and DCR, both in the as-hardened state and after heat treatments at 900 and 1100 °C.

DCR was found to produce a depth of cold work greater by a factor of three. It was approximately three times less severe per unit of depth than that produced by MSP. Both procedures resulted in multiple sets of slip bands, with those arising from DCR being much more widely spaced.

RX grains formed on the sample surfaces after both heat treatments, with DCR displaying lower RX depths than MSP, and the treatment at 1100 °C producing deeper RX. At 900 °C, TCP precipitates formed on slip bands in both samples, up to ~half the depth of cold work.

After the 1100 °C heat treatment, the microstructures of both samples underwent rafting, with peak rafting occurring beyond the depth of cold work. The depth at which the rafting occurred below the surface correlated well with the depth of compressive residual stress in each sample, showing that residual stress promotes rafting, while cold work retards it.

References

[1] H. Long, S. Mao, Y. Liu, Z. Zhang, X. Han, *Microstructural and compositional design of Ni-based single crystalline superalloys — A review*, Journal of Alloys and Compounds, Vol. 743 (2018) pp. 203–220.

[2] C.C. Wong, A. Hartawan, W.K. Teo, *Deep cold rolling of features on aero-engine components*, Procedia CIRP, Vol. 13 (2014) pp. 350–354.

[3] G.J. Gibson, K.M. Perkins, S. Gray, A.J. Leggett, *Influence of shot peening on high-temperature corrosion and corrosion-fatigue of nickel based superalloy 720Li*, Materials at High Temperatures, Vol. 33 (2016) pp. 225–233.

[4] B. Nagarajan, D. Kumar, Z. Fan, S. Castagne, *Effect of deep cold rolling on mechanical properties and microstructure of nickel-based superalloys*, Materials Science and Engineering A, Vol. 728 (2018) pp. 196–207.

[5] J. Hoffmeister, V. Schulze, A. Wanner, R. Hessert, G. Koenig, *Thermal relaxation of residual stresses induced by shot peening in IN718*, 10th International Conference on Shot Peening (2008) pp. 157–162.

[6] H.L. Cockings, B.J. Cockings, W. Harrison, M. Dowd, K.M. Perkins, M.T. Whittaker, G.J. Gibson, The effect of near-surface plastic deformation on the hot corrosion and high temperature corrosion-fatigue response of a nickel-based superalloy, Journal of Alloys and Compounds, Vol. 832 (2020) art. 154889.

[7] S.I. Wright, M.M. Nowell, D.P. Field, *A review of strain analysis using electron backscatter diffraction*, Microscopy and Microanalysis, Vol. 17 (2011) pp. 316–329.

[8] I. Bogachev, K.M. Knowles, G.J. Gibson, Electron backscattered diffraction analysis of cold work in a shot peened single crystal nickel superalloy, Materialia, Vol. 14 (2020) art. 100860.

[9] D.C. Cox, B. Roebuck, C.M.F. Rae, R.C. Reed, *Recrystallisation of single crystal superalloy CMSX–4*, Materials Science and Technology, Vol. 19 (2003) pp. 440–446.

[10] Z. Zhang, Z. Yue, TCP phases growth and crack initiation and propagation in nickel-based single crystal superalloys containing Re, Journal of Alloys and Compounds, Vol. 746 (2018) pp. 84–92.

[11] H. Biermann, U. Tetzlaff, H. Mughrabi, B. Grossmann, S. Mechsner, T. Ungár, *Investigations on the origin and effect of anomalous rafting*, Ninth International Symposium on Superalloys (2000) pp. 525–534.

[12] N. Matan, D.C. Cox, C.M.F. Rae, R.C. Reed, *On the kinetics of rafting in CMSX-4 superalloy single crystals*, Acta Materialia, Vol. 47 (1999) pp. 2031–2045.